ISSN 1392–1320 MATERIALS SCIENCE (MEDŽIAGOTYRA). Vol. 25, No. 3. 2019

Microstructure and Tribological Properties of Micro-arc Oxidation TiO_2 Coating Before and After SiC Particles Incorporation

Limei REN [1, 2], Tengchao WANG [1, 2], Zhaoxiang CHEN [2] *, Xipeng REN [2], Xiaowen QI [2]

[1] *Key Laboratory of Advanced Forging & Stamping Technology and Science (Yanshan University), Ministry of Education of China, Qinhuangdao City, 066004, PR China*
[2] *School of Mechanical Engineering, Yanshan University, Qinhuangdao City, 066004, PR China*

crossref http://dx.doi.org/10.5755/j01.ms.25.3.20089

Received 02 February 2018; accepted 25 April 2018

In this work, porous TiO_2 coating was fabricated on the surface of commercially pure titanium using the micro-arc oxidation (MAO) technique, and the effect of SiC particles incorporation on the microstructure and tribological properties of MAO TiO_2 coating was investigated. Results show that submicron SiC particles dispersed in the MAO electrolyte were incorporated into the TiO_2 coating during the MAO process and the fabricated TiO_2/SiC composite coating mainly consisted of rutile, anatase and SiC phases. The pore size and surface roughness of TiO_2/SiC composite coating decreased with the increasing addition amount of SiC particles in the electrolyte. Furthermore, the incorporation of SiC particles in the TiO_2 coating suppressed the initiation and propagation of micro-cracks. The tribological test of coatings against GCr15 stainless steel balls show that the incorporation of submicron SiC particles in the MAO TiO_2 coating decreased the friction coefficient and wear rate.

Keywords: titanium, micro-arc oxidation, SiC particles, composite coating, tribological property.

1. INTRODUCTION

Titanium and its alloys are widely used in aerospace, navigation and biomedical industries due to their high specific strength, excellent corrosion resistance and good biocompatibility. However, they have low surface hardness and poor wear resistance which may lead to premature failure of titanium components, thus severely limiting their application in the machinery and drive system [1].

Therefore, various surface techniques have been developed to strengthen surface mechanical performance of titanium alloys, including laser surface remelting [2], plasma nitriding [3], heat treatment [4], etc. In recent years, micro-arc oxidation (MAO) treatment of titanium alloys is gaining more and more attention because the fabricated MAO coating exhibits increased surface hardness and good adhesion strength. This technique is based on anodic oxidation of valve metals in a suitable electrolyte. As the anodization voltage increases up to the occurrence of plasma micro-arc discharges, the porous coating in-situ grows on the metal surface under the combined action of instantaneous high temperature and high pressure [5]. However, this fabrication process usually results in high porosity and surface roughness of the MAO coating which causes a high friction coefficient and relatively low wear resistance under non-lubrication conditions [6].

In order to improve the tribological performance of MAO coatings, researchers dispersed functional particles in the MAO electrolyte and attempted to incorporate these particles into the MAO coating during the anodization process [7, 8]. For example, the Si_3N_4/TiO_2 composite coating was fabricated on the pure titanium by directly adding Si_3N_4 particles into the electrolyte and the tribological performance of MAO coating was effectively improved [9]. Silicon carbide (SiC) has a wide range of application in the industrial field because of its advantages such as high hardness, stable chemical properties, high thermal conductivity and excellent abrasion resistance [10]. Therefore, it is reasonable to speculate that incorporating of SiC particles into the MAO coatings could contribute to improving the wear performance of composite coatings. And the relevant study on titanium and its alloy is seldom reported.

In this research, different amount of SiC submicron particles were added to phosphate-silicate based electrolytes to fabricate composite coatings on the surface of titanium. The microstructure, composition and tribological properties of MAO TiO_2 coating before and after the incorporation of SiC particles were investigated using SEM, XRD, confocal microscope, surface profiler and ball-on-plate tribometer test.

2. EXPERIMENTAL DETAILS

A commercially pure titanium plate, with a size of 25 mm × 80 mm × 1 mm, was used as the substrate for fabricating MAO ceramic coatings. Prior to MAO processing, all samples were ground with 1500-grit sandpapers and then cleaned with 95 % alcohol ultrasonically for 20 min. Then, all samples were cleaned with distilled water and dried in warm air.

The electrolyte consisted of Na_2SiO_3 (15 g/L), Na_3PO_4 (10 g/L) and NaOH (1 g/L). And the concentration of added SiC particles was 0 g/L, 4 g/L and 12 g/L, respectively. The average diameter of SiC particles (Shanghai Aladdin Bio-Chem Tech Co. LTD, China) was 0.5 ~ 0.7 μm, being at the

* Corresponding author. Tel.: +86-335-8068374; fax: +86-335-8077049.
E-mail address: *zxchen@ysu.edu.cn* (Z.X. Chen)

submicron scale. A pulsed asymmetric bipolar AC power supply (MAO120HD-III, Xi'an University of Technology, China) was employed to fabricate ceramic composite coatings on the titanium surface. The anodization of titanium was carried out under the mode of constant voltage. The MAO parameters are listed in Table 1. During the treatment, titanium samples and stainless steel plate were used as the anode and cathode, respectively. Air pump was opened to agitate the electrolyte and increase the dispersion of SiC particles. The electrolyte temperature was kept below 40 °C by a circulating cooling system.

Table 1. The parameters setting of MAO power supply

Parameter	Voltage	Frequency	Duty cycle	Time
Forward	420 V	500 Hz	35 %	20 min
Reverse	50 V	500 Hz	15 %	

The microstructure and chemical composition of coatings was investigated using scanning electron microscopy (SEM, SIGMA-500, ZEISS, Germany), equipped with energy dispersive spectroscopy (EDS). The phase structure of coatings was determined by thin-film X-ray diffraction (TF-XRD, D/MAX-2500/PC, RIGAKU, Japan). The TF-XRD measurement was carried out in the 2θ range of 20° ~ 80° at a scanning speed of 2 °/min. The surface roughness (Ra and Rz) of coatings was evaluated by a confocal microscope.

The friction coefficient and wear-resisting property of coatings were measured at room temperature under dry sliding condition by using a ball-on-plate reciprocating tribometer (Tribometer, Anton-Paar, Switzerland). The GCr15 stainless steel ball, with a diameter of 3 mm, was used as grinding ball in the test. The tribo-tests were carried out at a normal load of 3 N with a wear distance of 100 m. After the friction and wear tests, the wear tracks of samples was measured by using confocal microscope and the cross-section areas of wear tracks were tested by a surface profiler (MarSurf, Mahr, Germany). The wear rate K is calculated by using Eq. 1:

$$K = \frac{S \times l}{F \times L} \quad , \qquad (1)$$

where S is the cross-section areas of wear track, mm^2; l is the length of wear track, mm; F is the applied load, N; L is the sliding distance, m.

3. RESULTS AND DISCUSSION

3.1. Voltage-time responses

Fig. 1 presents the MAO voltage-time curves of titanium samples under the constant voltage mode in the electrolyte containing different concentrations of SiC submicron particles. At the beginning of the MAO treatment, the voltage increased linearly with time before the occurrence of plasma micro-arc discharges. A large number of small oxygen bubbles gathered on the surface of the titanium sample due to the electrolysis of water. The thickness of the coating increased quickly at this stage because of the rapid chemical reaction between the oxygen and titanium. Therefore the voltage increased with the increasing electrical resistance of the growing coating. After the plasma micro-arc discharges occurred, the increase of voltage became relatively slow and reached the final set value of 420 V.

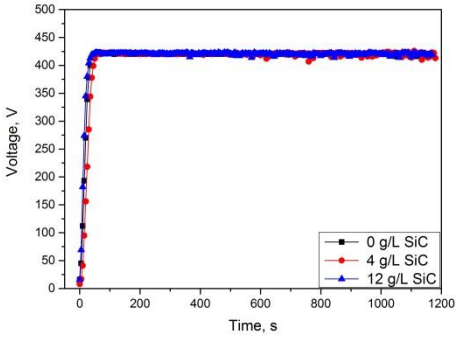

Fig. 1. MAO voltage-time curves of titanium samples in the electrolyte with different concentration of SiC particles

The MAO process was a complex reaction, which involved chemical oxidation, electrochemical oxidation and plasma electrolytic oxidation [11]. Generally, the addition of particles into the electrolyte had certain effects on the MAO process because these particles could change the conductivity and viscosity of electrolyte. Some studies showed that the addition of particles slowed down the MAO voltage ramp [12]. However, there were some other studies reported that the addition of particles had no significant influence on the MAO process [13]. In the present study, all samples treated in different concentrations of SiC submicron particles exhibited similar voltage-time curves (Fig. 1), demonstrating that adding submicron SiC particles into the electrolyte had no significant influence on the electrical characteristics of MAO process. The reason for this may be that the addition of a small quantity of SiC submicron particles into the electrolyte did not change the conductivity and pH value of the electrolyte significantly.

3.2. Microstructure and composition

Fig. 2 shows the surface morphologies of titanium substrate, particle-free MAO TiO_2 coating and TiO_2/SiC composite coatings fabricated in the electrolyte containing 4 g/L and 12 g/L SiC particles, respectively.

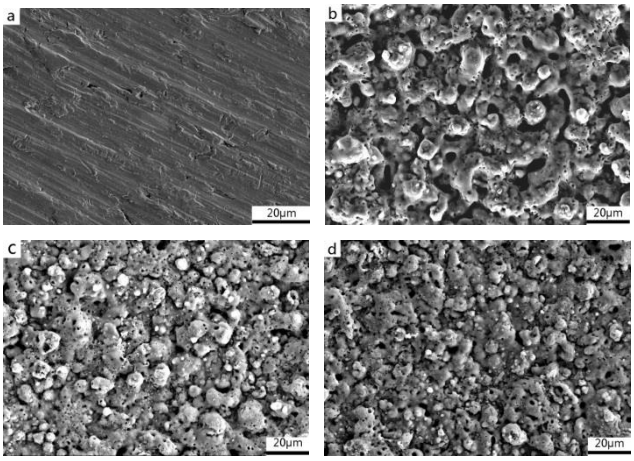

Fig. 2. Surface morphologies of the: a – titanium substrate; b – TiO_2 coating without SiC particles and TiO_2/SiC composite coatings fabricated in the electrolyte containing c – 4 g/L; d – 1 g/L SiC particles

The SEM image of titanium substrate ground by sandpapers is shown in Fig. 2 a. As shown in Fig. 2 c and d, the addition of SiC particles to the electrolyte had a significant influence on the microstructure of MAO coatings. Although the surface morphology of TiO_2/SiC composite coating fabricated in the electrolyte containing 4 g/L SiC particles was not significantly different from that of the particle-free TiO_2 coating due to the small addition amount of particles, the average pore size decreased and many particles were incorporated into the MAO coating surface.

When the concentration of SiC particles in the electrolyte was increased up to 12 g/L, the fabricated TiO_2/SiC composite coating became denser due to the sealing effect of SiC particles, as show in Fig. 2 d. The pore size was in the range of about 0.5 ~ 4 μm and decreased obviously in comparison with particle-free TiO_2 coating. Moreover, the TiO_2/SiC composite coating exhibited a relatively smoother surface. The element composition analysis of coatings by EDS show that the average Si content in the coatings fabricated in different electrolytes increased from 22.8 wt.% (electrolyte containing 0 g/L SiC) to 27.4 wt.% (electrolyte containing 4 g/L SiC) and 29.3 wt.% (electrolyte containing 12 g/L SiC). The existence of Si in the coating fabricated in the SiC particle-free electrolyte suggests that silicate anions in the electrolyte were incorporated into the oxide film during the MAO treatment of titanium. Similarly, the C content in the coatings increased with the increasing concentration of SiC particles in the electrolyte. These results indicated that adding SiC particles in the electrolyte influenced the formation, microstructure and composition of the MAO TiO_2 coating.

The XRD patterns of SiC particles, TiO_2 coating without SiC particles and TiO_2/SiC composite coatings fabricated in the electrolyte containing 4 g/L and 12 g/L SiC particles are shown in Fig. 3.

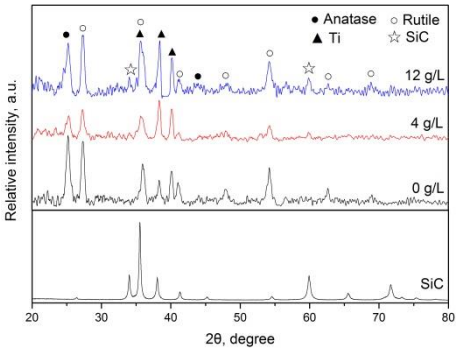

Fig. 3. XRD patterns of SiC particles, TiO_2 coating without SiC particles and TiO_2/SiC composite coatings fabricated in the electrolyte containing 4 g/L and 12 g/L SiC particles

The particle-free TiO_2 coating mainly consisted of anatase and rutile TiO_2. After adding SiC particles into the electrolyte, a new phase of SiC can be detected in the fabricated MAO coatings. This result was consistent with the SEM observation shown in Fig. 2 c and d, indicating that SiC particles in the electrolyte were successfully incorporated into the MAO TiO_2 coatings. During the MAO process, SiC particles were deposited into the TiO_2 coating under the action of electrophoretic, diffusion and adsorption [11], either filling into the coating micro-pores or being captured by the molten coating materials. In addition, it can be seen from XRD pattern that the relative peak intensity of rutile TiO_2 versus anatase TiO_2 increased after the incorporation of SiC particles. This is because the adding of SiC particles in the MAO electrolyte decreased the thermal conductivity of electrolyte, which promoted unstable anatase TiO_2 phase to transform into stable rutile TiO_2 phase under higher temperature.

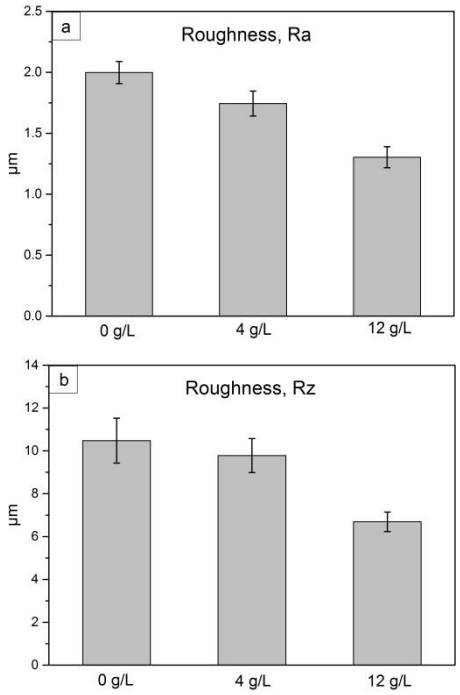

Fig. 4. Surface roughness Ra (a) and Rz (b) of MAO coatings fabricated in the electrolytes with different concentration of SiC particles

Fig. 4 shows the effect of SiC particle incorporation on the surface roughness of MAO coatings. The surface roughness of the MAO coatings decreased gradually with the increasing concentrations of SiC particles. For the TiO_2/SiC composite coating fabricated in the electrolyte containing 4 g/L SiC particles, the surface roughness decreased slightly compared with the particle-free MAO coating due to the small addition amount of particles. In contrast, a significant decrease in surface roughness can be observed for the TiO_2/SiC composite coating fabricated in the electrolyte containing 12 g/L SiC particles. To be specific, both the Ra and Rz values of the TiO_2/SiC composite coating are about 35 % lower than that of the particle-free coating. Such a significant decrease in surface roughness resulted from the filling effect of SiC particles during the MAO process.

The high magnification SEM images of the surface and cross-sectional morphologies of MAO coatings are shown in Fig. 5. For the TiO_2 coating without SiC particles, there were many micro-cracks existing on the coating surface, especially around the discharge channels (Fig. 5 a). The cross-sectional SEM observation reveals that some micro-cracks had penetrated through the entire coating in the thickness direction and began to propagate along the coating/substrate interface. These cracks would have a detrimental impact on the coating strength and its adhesion to the substrate (Fig. 5 b). The formation and propagation of these micro-cracks were mainly caused by the following

reasons. First, the MAO reaction was an intense and complex reaction accompanied with local instantaneous high temperature due to plasma micro-arc discharges and rapid cooling of the coating caused by the circulating electrolyte. Thus, the MAO ceramic coating, with lower coefficient of thermal expansion compared with titanium substrate, suffered from temperature changes intensively and frequently, which promoted the initiation and propagation of cracks greatly. In addition, the brittle nature, porous structure and high growth stress of the MAO coating also contributed to the crack formation.

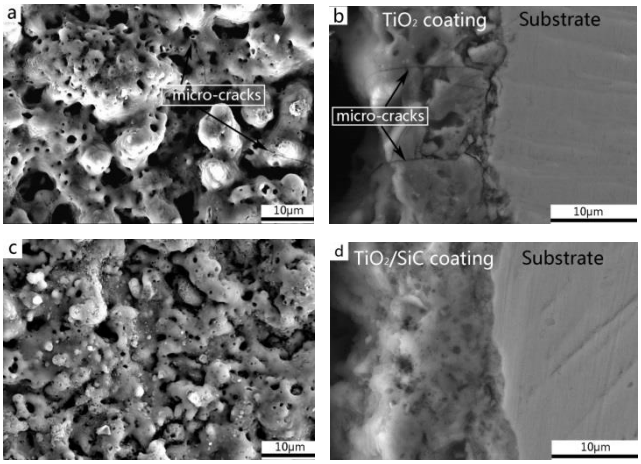

Fig. 5. Surface and cross-sectional morphologies of the (a, b) TiO_2 coating without SiC particles and (c, d) TiO_2/SiC composite coating fabricated in the electrolyte containing 12 g/L SiC particles

On the other hand, there were no significant micro-cracks being observed on the surface of TiO_2/SiC composite coating, as shown in Fig. 5 c. This is because that incorporating the second phase particles into the matrix of brittle ceramic materials can improve the fracture toughness of the ceramic coating. These particles dispersed in the coating effectively inhibited the initiation and propagation of micro-cracks [16]. Comparing Fig. 5 b and d, it can be seen that there was no obvious thickness difference between TiO_2 coating and TiO_2/SiC composite coating. The reason for this phenomenon was that they had similar voltage-time responses (Fig. 1) [17].

In addition, the cross-section morphology of particle-free TiO_2 coating revealed some surface-connected channels and internal pores, as shown in Fig. 5 b. These patterns are the typical feature of the MAO coating. After incorporating SiC particles in TiO_2 coating, the cross-sectional structure of the coating became denser due to the filling effect of SiC particles (Fig. 5 d).

3.3. Tribological properties

The tribological properties of titanium substrate, TiO_2 coating and TiO_2/SiC composite coatings were measured at room temperature under dry sliding condition by using a ball-on-plate reciprocating tribometer. The tribo-tests were carried out at a normal load of 3 N with a GCr15 stainless steel ball as the grinding ball. The relationship between the friction coefficient and sliding distance of various samples is shown in Fig. 6.

For the titanium substrate, the friction coefficient climbed up to an average value of about 0.52 with significant fluctuations after the initial decrease (see curve a in Fig. 6). For the MAO TiO_2 coating, the friction coefficient curve (see curve b in Fig. 6) exhibited relatively higher value (about 0.71) throughout the whole sliding distance. As shown in section 3.2, the MAO TiO_2 coating had complex surface and internal microstructure (see Fig. 2 b and Fig. 5 b). Both its surface features (high surface roughness and widespread surface craters/ravines) and cross-sectional features (penetrating micro-cracks and internal pores) contributed to the unstable contact between the TiO_2 coating and the GCr15 ball, thus resulting in fluctuating and high friction coefficient.

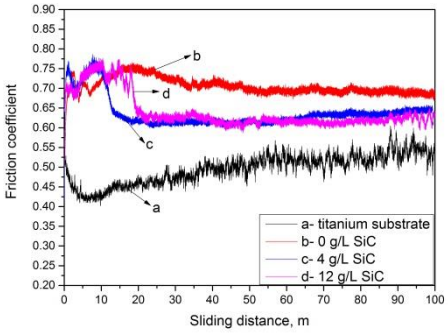

Fig. 6. The relationship between the friction coefficient and sliding distance of titanium substrate and MAO coatings fabricated in the electrolytes with different concentration of SiC particles

From curve c and d in Fig. 6, it can be seen that the friction coefficient curves of TiO_2/SiC composite coatings against GCr15 ball exhibited significant fluctuations only at the initial stage of the tribo-tests. After the initial sliding distance of about 20 m, the friction coefficient decreased and became relatively stable (about 0.62) for both kinds of TiO_2/SiC composite coatings. Take the coating sample fabricated in the electrolyte containing 12 g/L SiC particles for example, although it had a rough and porous surface similar to the MAO TiO_2 coating (see Fig. 2 b and d), its cross-sectional microstructure was relatively denser than that of the TiO_2 coating due to the sealing effect of SiC particles (see Fig. 5 b and d). The surface microstructure of TiO_2/SiC composite coatings caused the initial fluctuation of friction coefficient. As the rough and porous surface layer of the TiO_2/SiC composite coating being worn off, the GCr15 ball began to contact with the denser and harder inner layer of the composite coating, thereby resulting in decreased and stable friction coefficient.

Table 2. The element composition of worn surface of TiO_2/SiC composite coating

Element, wt.%	C	O	Na	Si	P	Ti	Cr	Fe
S1	9.86	38.59	0.26	21.52	1.92	22.73	–	5.11
S2	4.93	40.26	–	2.79	–	3.27	0.68	48.07

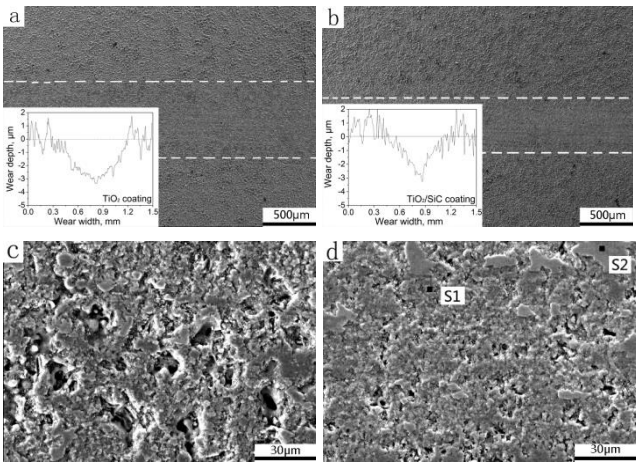

Fig. 7. Wear track profiles and worn morphologies of the (a, c) TiO_2 coating without SiC particles and (b, d) TiO_2/SiC composite coating fabricated in the electrolyte containing 12 g/L SiC particles after a sliding distance of 100 m

Fig. 7 exhibits the wear track profiles and macro/micro worn morphologies of the TiO_2 coating without SiC particles and TiO_2/SiC composite coating fabricated in the electrolyte containing 12 g/L SiC particles after a sliding distance of 100 m. From the wear track profiles and the macro worn morphologies of two coatings (see Fig. 7 a and b), it can be noticed that the wear track width of the TiO_2/SiC composite coating was much smaller than that of particle-free TiO_2 coating. This means that the incorporation of the SiC particles strengthened the surface wear-resisting performance of the TiO_2 coating. Comparing the micro worn morphologies of two coatings (Fig. 7 c and d), it can be seen that there were still lots of pores on the worn surface of the particle-free TiO_2 coating after the tribo-test (Fig. 7 c), demonstrating high porosity both in its surface and interior. The porous structure and the existence of micro-cracks weakened the strength and toughness of TiO_2 coating greatly so that a significant amount of coating materials were worn off under the action of tangential grinding force, resulting in wider wear track. In contrast, there were only a small number of pores being observed on the worn surface of the TiO_2/SiC composite coating (Fig. 7 d), indicating its relatively denser internal structure, higher hardness and fracture toughness. Additionally, it can be seen from Fig. 7 c and d that there were two kinds of typical worn surface morphologies. The element composition of worn surface of TiO_2/SiC composite coating fabricated with 12 g/L SiC particles was analyzed by EDS and the results were listed in Table 2. The first worn morphology resulted from abrasive wear, as marked by S1 in Fig. 7 d. The main chemical element in this area (S1) was O, Ti and Si (see Table 2). The wear mechanism of the MAO coating was governed by abrasive wear. At the initial stage of tribo-test, the brittle and porous surface layer of the MAO coating were crushed under the normal loading and formed lots of oxide debris. During the subsequent tribo-test, the oxide debris caused abrasive wear between the MAO coating and GCr15 ball. For the second worn morphology, some smooth areas were observed on the worn trace, as marked by S2 (see Fig. 7 d). In this area (S2), a lot of Fe and O elements as well as small quality of Cr element were detected (see Table 2), indicating that materials were transferred from GCr15 ball to the MAO coating surface and ferrous oxides formed during the wear process. This phenomenon demonstrated the occurrence of adhesive wear. The wear debris derived from GCr15 ball were repeatedly smeared on the coating surface and formed a mechanically mixed area during the wear process. As a result, the sliding pairs in this area were changed from GCr15 versus MAO coating to GCr15 versus mixing layer.

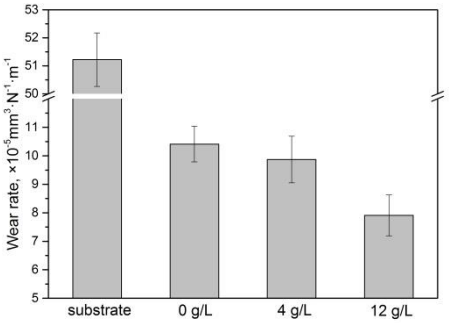

Fig. 8. Wear rate of titanium substrate and MAO coatings fabricated in the electrolytes with different concentration of SiC particles

As shown in Fig. 8, the titanium substrate exhibited the highest wear rate and the average wear rate of coatings decreased with the increasing concentration of SiC particles in the electrolyte (from 10.4×10^{-5} $mm^3 \cdot N^{-1} \cdot m^{-1}$ of the TiO_2 coating to 7.9×10^{-5} $mm^3 \cdot N^{-1} \cdot m^{-1}$ of the TiO_2/SiC composite coating fabricated with 12 g/L SiC particles). The result was consistent with the surface worn morphology shown in Fig. 7. This means the incorporation of SiC submicron particles can effectively reduce the wear rate of MAO coatings. The wear resistance of the MAO coatings was directly related to its hardness, internal defect and friction coefficient. The combined effects of decreasing friction coefficient and increasing mechanical properties due to the filling effect of SiC particles are the main reasons for the remarkable improvement of wear resistance. For one thing, the micro-pores of the MAO coating were filled with SiC submicron particles to form a dense structure with low friction coefficient. For another, the dispersed SiC particles in the matrix of composite coating have the functions of pinning and strengthening, which improves the mechanical properties of the MAO coating. In addition, the incorporation of SiC particles in MAO coating effectively suppressed micro-cracks formation and decreased the coating internal defects.

4. CONCLUSIONS

The TiO_2/SiC composite coating was successfully fabricated by the micro-arc oxidation treatment of titanium in the electrolyte containing SiC submicron particles. The surface micro-pore size and roughness of coatings decreased with the increasing concentration of SiC particles in the electrolyte. The average Si content in the fabricated coatings increased from 22.8 wt.% to 29.3 wt.% before and after the addition of 12 g/L SiC particles in the electrolyte. The incorporation of SiC submicron particles in the coatings suppressed the initiation and propagation of micro-cracks.

The TiO_2/SiC composite coating exhibited lower friction coefficient (about 0.62) than that of TiO_2 coating (about 0.71). The average wear rate of TiO_2/SiC coating

fabricated in the electrolyte containing 12 g/L SiC particles was 7.9×10^{-5} $mm^3 \cdot N^{-1} \cdot m^{-1}$, which was smaller than that of SiC particle-free TiO_2 coating (10.4×10^{-5} $mm^3 \cdot N^{-1} \cdot m^{-1}$).

Acknowledgments

This work is supported by Natural Science Foundation (E2016203270), Returned Overseas Chinese Talents Foundation (CL201726), Civil-military Integration Industry Development Foundation (2017B110) of Hebei Province, and Fundamental Research Foundation (020000904) and Doctoral Foundation (B942) of Yanshan University.

REFERENCES

1. **Mogonye, J.E., Scharf, T.W.** Tribological Properties and Mechanisms of Self-Mated Ultrafine-Grained Titanium *Wear* 376 2017: pp. 931 – 939. https://doi.org/10.1016/j.wear.2016.10.016
2. **Yao, Y., Li, X., Wang, Y.Y., Zhao, W., Li, G., Liu, R.P.** Microstructural Evolution and Mechanical Properties of Ti-Zr Beta Titanium Alloy after Laser Surface Remelting *Journal of Alloys and Compounds* 583 2014: pp. 43 – 47. https://doi.org/10.1016/j.jallcom.2013.08.160
3. **Ossowski, M., Borowski, T., Tarnowski, M., Wierzchon, T.** Cathodic Cage Plasma Nitriding of Ti6Al4V Alloy *Materials Science (Medžiagotyra)* 22 (1) 2016: pp. 25 – 30. http://dx.doi.org/10.5755/j01.ms.22.1.7343
4. **Fomin, A., Dorozhkin, S., Fomina, M., Koshuro, V., Rodionov, I., Zakharevich, A., Petrova, N., Skaptsov, A.** Composition, Structure and Mechanical Properties of the Titanium Surface after Induction Heat Treatment Followed by Modification with Hydroxyapatite Nanoparticles *Ceramics International* 42 (9) 2016: pp. 10838 – 10846. https://doi.org/10.1016/j.ceramint.2016.03.213
5. **Dou, J.H., Chen, Y., Yu, H.J., Chen, C.Z.** Research Status of Magnesium Alloys by Micro-arc Oxidation: A Review *Surface Engineering* 33 (10) 2017: pp. 731 – 738. https://doi.org/10.1080/02670844.2017.1278642
6. **Li, Z., Di, S.** Preparation and Properties of Micro-Arc Oxidation Self-lubricating Composite Coatings Containing Paraffin *Journal of Alloys and Compounds* 719 2017: pp. 1 – 14. https://doi.org/10.1016/j.jallcom.2017.05.138
7. **Lu, X., Mohedano, M., Blawert, C., Matykina, E., Arrabal, R., Kainer, K.U., Zheludkevich, M.L.** Plasma Electrolytic Oxidation Coatings with Particle Additions-A Review *Surface and Coatings Technology* 307 2016: pp. 1165 – 1182. https://doi.org/10.1016/j.surfcoat.2016.08.055
8. **Hakimizad, A., Raeissi, K., Golozar, M.A., Lu, X., Blawert, C., Zheludkevich, M.L.** The Effect of Pulse Waveforms on Surface Morphology, Composition and Corrosion Behavior of Al_2O_3 and Al_2O_3/TiO_2 Nano-Composite PEO Coatings on 7075 Aluminum Alloy *Surface and Coatings Technology* 324 2017: pp. 208 – 221. https://doi.org/10.1016/j.surfcoat.2017.05.068
9. **Aliofkhazraei, M., Sabour Rouhaghdam, A., Shahrabi, T.** Abrasive Wear Behaviour of Si_3N_4/TiO_2 Nanocomposite Coatings Fabricated by Plasma Electrolytic Oxidation *Surface and Coatings Technology* 205 2010: pp. S41 – S46. https://doi.org/10.1016/j.surfcoat.2010.03.052
10. **Wu, R., Zhou, K., Yue, C.Y., Wei, J., Pan, Y.** Recent Progress in Synthesis, Properties and Potential Applications of SiC Nanomaterials *Progress in Materials Science* 72 2015: pp. 1 – 60. https://doi.org/10.1016/j.pmatsci.2015.01.003
11. **Shokouhfar, M., Allahkaram, S.R.** Formation Mechanism and Surface Characterization of Ceramic Composite Coatings on Pure Titanium Prepared by Micro-Arc Oxidation in Electrolytes Containing Nanoparticles *Surface and Coatings Technology* 291 2016: pp. 396 – 405. https://doi.org/10.1016/j.surfcoat.2016.03.013
12. **Wang, Y., Wei, D., Yu, J., Di, S.** Effects of Al_2O_3 Nano-additive on Performance of Micro-Arc Oxidation Coatings Formed on AZ91D Mg Alloy *Journal of Materials Science & Technology* 30 (10) 2014: pp. 984 – 990. https://doi.org/10.1016/j.jmst.2014.03.006
13. **Arrabal, R., Matykina, E., Viejo, F., Skeldon, P., Thompson, G.E., Merino, M.C.** AC Plasma Electrolytic Oxidation of Magnesium with Zirconia Nanoparticles *Applied Surface Science* 254 (21) 2008: pp. 6937 – 6942. https://doi.org/10.1016/j.apsusc.2008.04.100
14. **Chen, Z.X., Wang, W.X., Takao, Y., Matsubara, T., Ren, L.M.** Microstructure and Shear Fracture Characteristics of Porous Anodic TiO_2 Layer before and after Hot Water Treatment *Applied Surface Science* 257 (16) 2011: pp. 7254 – 7262. https://doi.org/10.1016/j.apsusc.2011.03.101
15. **Chen, Z.X., Wang, W.X., Takao, Y., Matsubara, T., Ren, L.M.** Characterization and Fatigue Damage of TiO_2 Layer on Spark-Anodized Titanium before and after Hot Water Treatment *Applied Surface Science* 262 2012: pp. 2 – 7. https://doi.org/10.1016/j.apsusc.2011.11.111
16. **Giang, N.A., Kuna, M., Hütter, G.** Influence of Carbide Particles on Crack Initiation and Propagation with Competing Ductile-Brittle Transition in Ferritic Steel *Theoretical and Applied Fracture Mechanics* 92 2017: pp. 89 – 98. https://doi.org/10.1016/j.tafmec.2017.05.015
17. **Bahramian, A., Raeissi, K., Hakimizad, A.** An Investigation of the Characteristics of Al_2O_3/TiO_2 PEO Nanocomposite Coating *Applied Surface Science* 351 2015: pp. 13 – 26. https://doi.org/10.1016/j.apsusc.2015.05.107